

# Solitary wave solutions as a signature of the instability in the discrete nonlinear Schrödinger equation

Edward Arévalo

*Technische Universität Darmstadt, Institut für Theorie elektromagnetischer Felder,  
TEMF, Schloßgartenstr. 8 D-64289 Darmstadt, Germany*

(Dated: October 30, 2018)

## Abstract

The effect of instability on the propagation of solitary waves along one-dimensional discrete nonlinear Schrödinger equation with cubic nonlinearity is revisited. A self-contained quasicontinuum approximation is developed to derive closed-form expressions for small-amplitude solitary waves. The notion that the existence of nonlinear solitary waves in discrete systems is a signature of the modulation instability is used. With the help of this notion we conjecture that instability effects on moving solitons can be qualitative estimated from the analytical solutions. Results from numerical simulations are presented to support this conjecture.

PACS numbers: 05.45.Yv, 05.45.-a, 63.20.Ry

Keywords: discrete nonlinear Schrödinger equation, solitons, Modulation stability analysis

## I. INTRODUCTION

The discrete nonlinear Schrödinger equation (DNLSE) is one of the most investigated systems in dynamical nonlinear lattices. In particular the DNLSE with cubic nonlinearity is an ubiquitous dynamical-lattice system which has been extensively studied because its direct physical applications, such as Bose-Einstein condensates (BECs) in deep optical lattices or optical beams in waveguide arrays, among others. In particular, the transport properties of neutral atoms in BEC arrays has gained interest in the last few years [1] due, in principle, to the possible technological applications as matter-wave interferometry [2] or quantum information processing [3, 4].

Of course, solitary waves are promising candidates for the coherent matter wave transport in BEC arrays. Notice that, in the strict sense, solitons (defined as solitary waves that maintain their shape and amplitude owing to a self-stabilization against diffraction through a nonlinear interaction) do not exist in the DNLSE. It is because the DNLSE is a nonintegrable system. However, approximate moving solitary-wave solutions can be analytically calculated. One of the main characteristic of these waves is that they emit radiation when moving, and eventually become pinned by the lattice [5]. This is a radiative deceleration which is extremely slow [5], and therefore do not play a role in the present analysis.

In the following we shall use a weak definition of soliton to refer to solitary wave solutions following from approximate integration of the DNLSE.

We note that diverse analytical approximations have been developed in the last two decades to obtain moving solitary wave solutions of the DNLSE for bright solitons (the theory of the perturbed Ablowitz-Ladik equation [6, 7, 8, 9, 10], iteration methods [11], semi-discrete approximation [12], variational approximation [9, 13], or an explicit perturbation theory [5, 11, 14]) as well as for dark solitons (quasicontinuum approximation [15], or by construction [16, 17]). Of course, the DNLSE in the continuum approximation leads to the standard nonlinear Schrodinger equation (NLSE). Notice, however, that the soliton solutions of the NLSE do not move along the lattice, i.e. they behave as breathers in the DNLSE system.

In the absence of dissipation and inhomogeneities [13, 18, 19, 20, 21] and taking into account that radiative deceleration is very slow [5] the main effect which reduces the life duration of these solitary waves is the instability of the system. The instability effect in

moving solitons manifests itself as a distortion of exponential-like nature of the envelope during propagation [14].

It is a common notion in discrete systems that solitons exist or can be excited in the region of parameters where modulation instability (MI) of planewaves appears [7, 22, 23, 24]. So, solitons by themselves can be considered as a signature of the MI. Moreover, since the MI is a permanent feature of the discrete system, i.e. it does not disappear after the appearance of solitons, it is reasonable to *conjecture* that the continuous deformation of moving solitons and breathers after formation is a MI effect.

The usual analytical procedure for studying MI effect on lattices is performing modulation stability analysis of planewaves [7, 17, 22, 23, 24, 25]. From this analysis usually qualitative conclusions are derived for solitons. Recently the stability of narrow discrete modes in the DNLSE was studied for the case  $JU < 0$  in Eq. (1) [26].

Since solitons can be considered a signature of the MI effect in discrete systems [7, 22, 23, 24], it is natural to conjecture that approximate analytical forms of the soliton solutions may contain already qualitative information of the MI (e.g. strength and parameter region of existence). Here, the MI strength refers to the grade of how during the time evolution the MI effect distorts the initial analytical soliton solution.

In the present study we are interested in studying anew the the stability of moving solitons in the DNLSE with the help of approximate analytical soliton solutions. In order to find these analytical soliton solutions we use a *self-contained* quasicontinuum approximation (SCQCA). Our aim is to show that these approximate analytical soliton solutions can be used to derive qualitative conclusions of the soliton stability in the range of parameters where the solutions are valid. In this regard we show that the amplitudes of these soliton solutions define an analytical upper boundary for a “self-defocusing” instability not only for bright but also for the dark solitons. Here the term “self-defocusing” instability refers to a decaying amplitude in moving solitons which also undergo width broadening. Numerical results supporting the analysis are presented. The standard modulation stability analysis is also revisited for comparison issues.

We want to comment that it may sound superfluous to propose another method for calculating solitary waves in the DNLSE since other powerful methods as, e.g. those propose in Refs. [5, 14], have already captured in fine detail interesting aspects of this equation. However, in contrast to those methods, the SCQCA can be straightforwardly extended to

two [31] and three spatial dimensions, where no other analytical methods for moving solitons have been proposed so far. Therefore, understanding the effect of the modulation instability on the solutions presented here is important in order to proceed to higher dimensions.

## II. THE SCQCA

### A. the DNLSE

The DNLSE with cubic nonlinearity, which is the basic model for the one-dimensional BEC arrays in the tight binding limit [13, 18, 19, 21], reads

$$i\partial_t\psi_n(t) + J(\psi_{n-1}(t) + \psi_{n+1}(t)) - U|\psi_n(t)|^2\psi_n(t) = 0, \quad (1)$$

where  $\psi_n$  is a complex amplitude of the BEC mean field at the site  $n$ ,  $J$  is proportional to the tunneling rate [13, 18, 19, 20, 21] and the nonlinear coefficient  $U$ , known also as the interaction strength. We note that Eq. (1) can be written in a dimensionless form. However, since we are interested in the sign effect of the nonlinear coefficient  $U$  we keep both parameters of Eq. (1) in our analysis.

Equation (1) is a simple model which reflects generic features of one-dimensional BEC arrays with homogeneous scattering length. The effects of dissipation and inhomogeneities are neglected [13, 18, 19, 20, 21]. Expressions for  $J$  and  $U$  are known and depend, among others, on the lattice spacing, the depth of the optical lattice, the  $s$ -wave scattering length, and the mass and number of the atoms [1, 13, 18, 19, 21]. These parameters can be manipulated in experiments to obtain different desirable configurations of the system. In particular the interaction strength  $U$  can be tuned through the  $s$ -wave scattering length, from positive values (repulsive interactions) to negative values (attractive interactions) by using either magnetic or laser fields.

### B. Soliton solutions

In the following we outline the SCQCA for the DNLSE in the spirit of Ref. [27, 28, 29, 30] to obtain approximate analytical soliton solutions. As mentioned above, the DNLSE is a nonintegrable system, i.e. not exact soliton solutions exist. Of course, the solitary solutions derived below are only approximations, since SCQCA is only an approximate integration of

the DNLSE. We note, to the best of our knowledge, that this SCQCA [27, 28, 29, 30] has not been applied to the DNLSE. The importance of this method resides in the fact that it can be used without resorting to the knowledge of other nonlinear partial differential equations. Therefore it is self-contained.

In order to proceed with the SCQCA we consider a travelling wave ansatz for an envelope complex function reading as

$$\psi_n(t) = \sum_{m=1}^{\infty} \chi_m(z) \exp(im\theta), \quad (2)$$

where  $z = n - v_0 v_k t$  and  $\theta = k n - \epsilon_0 E_k t + \delta$ . Here,  $k$  is the quasimomentum,  $v_k$  is a velocity,  $E_k$  is the particle energy,  $\delta$  is a phase, and both  $v_0$  and  $\epsilon_0$  are constants.

By using the full Taylor expansion of the function ( $\psi_{n\pm 1} \rightarrow \exp(\pm \partial_n) \psi_n$ ), Eq. (1) is transformed into an operator equation,

$$i\partial_t \psi_n(t) + 2J \cos(\partial_n) \psi_n(t) - W_n(t) = 0, \quad (3)$$

where  $W_n(t) = U|\psi_n(t)|^2 \psi_n(t)$ . Inserting the ansatz Eq. (2) in Eq. (3) and Fourier transforming the resultant equation we get

$$\tilde{W}_m(q) = a_m(q) \tilde{\chi}_m(q), \quad (4)$$

where

$$a_m(q) = 2J \cos(km + q) + m\epsilon_0 E_k + qv_0 v_k \quad (5)$$

Here tilde marks the Fourier transformed function, e.g.

$$\tilde{W}_m(q) = \frac{1}{\sqrt{2\pi}} \int_{-\infty}^{\infty} dz e^{iqz} W_m(z), \quad (6)$$

where  $W_m$  is an abbreviation which collect all products of envelope functions that belong to the same harmonic  $e^{im\theta}$ , i.e.

$$\sum_m W_m(z) e^{im\theta} = W_n \left( \sum_l \chi_l(z) e^{il\theta} \right). \quad (7)$$

The SCQCA consist in a formal solution of Eq. (4) for  $\tilde{W}_m(q)$  and in an expansion of the fraction  $a_m(q)$  (Eq. (5)) for small  $q$  [27, 28], i.e.  $a_m(q) \simeq \sum_n a_{nm} q^n$ . If we consider the expansion of the fraction  $a_m(q)$  up to second order in  $q$ , forcing the first order term of the

expansion to be zero by setting  $v_0 = 1$ , and transforming back to the position space, we find a second-order differential equation for the first harmonic  $\chi_1$ , namely

$$a_{01}\chi_1 - a_{21}\partial_z^2\chi_1 - 3U|\chi_1|^2\chi_1 = 0. \quad (8)$$

Integrating by parts Eq. (8) and integrating again leads to a solution for the envelope:

$$\psi_n^B(z) = 2\sqrt{\frac{J\cos(k)(\epsilon_0 - 1)}{-3U}} \operatorname{sech}\left(\sqrt{2}\sqrt{(\epsilon_0 - 1)}z\right) e^{i\theta}, \quad (9)$$

for  $JU\cos(k) < 0$  and  $\epsilon_0 > 1$  (bright soliton),

$$\psi_n^D(z) = \sqrt{2}\sqrt{\frac{J\cos(k)(\epsilon_0 - 1)}{-3U}} \tanh\left(\sqrt{1 - \epsilon_0}z\right) e^{i\theta}, \quad (10)$$

for  $JU\cos(k) > 0$  and  $\epsilon_0 < 1$  (dark soliton). From the SCQCA we obtain also that  $E_k = -2J\cos(k)$  and  $v_k = 2J\sin(k)$ . Notice that the range of high soliton velocity  $v_k$  (rapid solitons) corresponds to the values  $|k| \simeq \pi/2$ .

Here it is important to remark that Eqs. (9) and/or (10) satisfy the so called staggering transformation  $\psi_n \rightarrow (-1)^n \psi_n^*$  ( $\star$  stands for complex conjugation) [16], which has been widely used in the literature to consider the cases where the nonlinear coefficient  $U$  changes the sign. This transformation corresponds in Eqs. (9) and/or (10) to the case  $k \rightarrow \pi - k$ . The solutions that emerge after the transformation are similar to Eqs. (9) and/or (10) but with the sign in front of  $U$  changed. The conditions for the bright and dark regions are also interchanged, i.e.  $JU\cos(k) \rightarrow -JU\cos(k)$ . Notice, however, that with this transformation it is not possible to change from the bright region to the dark region or vice versa [equivalently, it is not possible to transform Eq. (9) into Eq. (10) or vice versa]. So, in the present case, it is not appropriate to infer conclusions from one region based on the information of the other region by simply using this transformation.

It is worth mentioning that the bright soliton solution, Eq. (9), is similar to that following from the perturbed Ablowitz-Ladik equation [6, 7, 8, 9, 10] only when  $\cos(k) = 1$  in the amplitude of Eq. (9). On the other hand, a dependence of the amplitude on the quasimomentum  $k$  was obtained for bright solitons in Ref. [5], but only for the case bright case ( $JU\cos(k) < 0$ ) in Eq. (1). In the case of dark solitons, this dependence was obtained in Ref. [15]. So far, the dependence of the soliton amplitudes on the function  $\cos(k)$  has not been analyzed in relation with their stability.

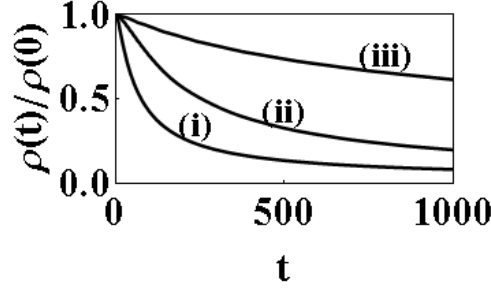


FIG. 1: Normalized probability-density maximum ,  $\rho(t)/\rho(0)$  [ $\rho(t) = \max(|\psi_n^B(t)|^2)$ ], of the bright soliton vs. the time  $t$ : (i)  $k = 0$  (or  $\pi$ ), (ii)  $k = 2\pi/5$  (or  $3\pi/5$ ), and (iii)  $k = 0.49\pi$  (or  $0.51\pi$ ) with  $J = 1$  and  $|U| = 1$ .

It is also good to keep in mind that a single dark soliton, Eq. (10), corresponds to the case where the sites of the BEC array are equally filled except in the region where the hole excitation is moving. However, one can construct pulse solitary waves in the dark region by subtracting two identical dark solitons separated some distance  $d > 0$  (see Figs. 5 and 6), i.e.

$$u_n = \psi_{n+d/2}^D(t) - \psi_{n-d/2}^D(t). \quad (11)$$

In the following we shall call  $u_n$  the dark pulse. Notice that the width of  $u_n$  depends not only on  $k$  but also on  $d$ . By choosing suitable values for  $d$  and  $\epsilon_0$  the form of dark pulses  $u_n$  can become very similar (but not equal) to the form of bright solitons.

### III. INSTABILITY EFFECT

In this section we first present a conjecture about how to estimate the instability effect on the moving solitons. Afterwards, with the help of numerical simulations we compare predictions from the well-known standard modulation stability analysis [7, 22, 23, 24] and from our conjecture. Special emphasis is done in the analysis of the dark region where the standard modulation stability analysis fails to predict analytically the instability of the system. We note that the instability of staggered dark solitons was numerically studied in Ref. [16].

Here we conjecture that the amplitudes of the approximate soliton solutions, Eqs. (9) and (10), contain qualitative information of the MI strength regardless of the soliton form. Since  $\epsilon_0$  and  $k$  are the free parameters of the system, they govern the MI strength on the

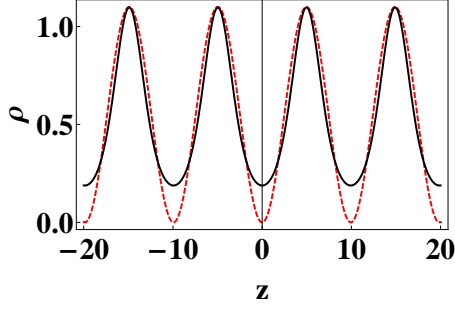


FIG. 2: Probability density of an infinity train of bright solitons (solid line), i.e.  $\rho = |\sum_j \psi_n^B(z - jL)|^2$ , compared with a modulation plane-wave  $\sin^2(Q)$  (dashed line). Here  $Q = \sqrt{(\epsilon_0 - 1)}$  and  $\epsilon_0 = 1.1$ . The amplitudes are normalized to one.

solitons. So, from a simple inspection of the amplitudes in Eqs. (9) and (10) we observe that the simplest common factor in both solutions containing  $\epsilon_0$  and  $k$  regardless of the signs is

$$\eta = \sqrt{|\cos(k)(\epsilon_0 - 1)|}. \quad (12)$$

The absolute value in Eq. (12) is used for convenience. Since  $\eta$  is proportional to the soliton amplitudes, we suppose that the MI strength regardless of the region [bright ( $JU \cos(k) > 0$ ) or dark ( $JU \cos(k) < 0$ )] is also proportional to  $\eta$ .

Notice that the magnitude of  $\eta$  reduces as  $|k| \rightarrow \pi/2$  vanishing exactly at  $|k| = \pi/2$  (maximum soliton velocity). So, here we can conjecture that MI for moving solitons is present in the whole first Brillouin zone except perhaps for  $|k| = \pi/2$ , i.e.  $|k| \in [0, \pi/2) \cup (\pi/2, \pi]$ . Moreover, since  $\eta$  increases as  $|\cos(k)| \rightarrow 1$ , we can conjecture also that the MI strength for moving solitons may increase and reach its maximum at  $|k| = 0, \pi$  (breather solutions) and may become weak as  $|\epsilon_0 - 1| \rightarrow 0$  (wide solutions). On the other hand, the MI effect on moving solitons can be expected regardless of the  $JU \cos(k)$  sign, since both approximate bright and dark soliton solutions have been derived.

The effect of MI on the small-amplitude soliton shapes [Eqs. (9) and (10)] is of “self-defocusing” nature, i.e. a broadening of the soliton width accompanied by exponential-like decay of the amplitude can be observed. As an example, in Fig. 1 it is shown the evolution of the normalized probability-density maximum of bright solitons for different values of the quasimomentum  $k$ . This figure shows that the MI strength can be characterized by studying the growth rate of the soliton amplitudes. Since in the present theory only defocusing MI



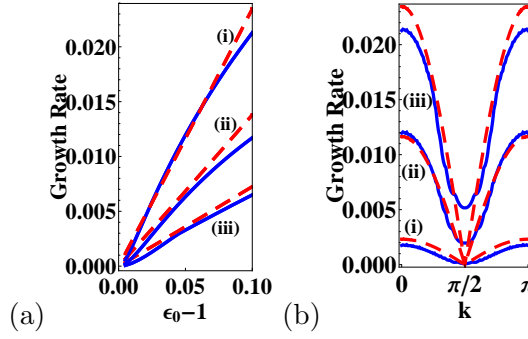


FIG. 3: (Color online) Growth rate for bright solitons,  $\psi_n^B$  [Eq.(9)]. a: Versus  $\epsilon_0 - 1$  for (i)  $k = 0$  (or  $\pi$ ), (ii)  $k = 3\pi/10$  (or  $7\pi/10$ ), (iii)  $k = 2\pi/5$  (or  $3\pi/5$ ). b: Versus  $k$  for (i)  $\epsilon_0 = 1.01$ , (ii)  $\epsilon_0 = 1.05$ , (iii)  $\epsilon_0 = 1.1$ . Numerical estimation  $\Gamma(T/2)$  with  $T = 10$  (solid line) and analytical estimation  $\kappa_1 \Im(E_Q)$  (dashed line).  $\kappa_1 = 0.4$  to fit numerical results.

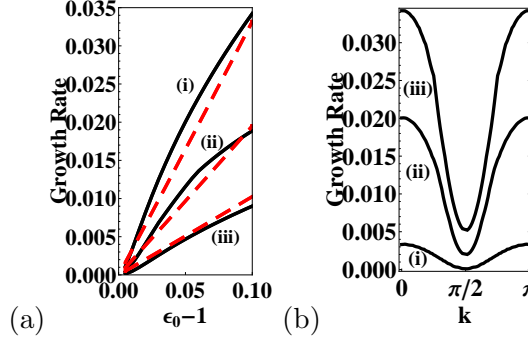


FIG. 4: (Color online) Numerical estimation of the Growth rate  $\Gamma(T/2)$  with  $T = 10$  (solid line) in the dark region for  $u^{test} = i\psi_n^B$  [ $i$  is the imaginary unit and  $\psi_n^B$  is given in Eq.(9)]. The same cases as in Fig. 3 are considered. In the panel (a) the analytical estimation for bright solitons  $\kappa_2 \Im(E_Q)$  (dashed lines) is also plotted with  $\kappa_2 = \sqrt{2}\kappa_1$  (see caption Fig. 3).

effect is observed, the growth rates for moving solitons are decaying [14].

We note that solitary waves with higher amplitudes than those of Eqs. (9) and (10) can undergo other MI effects as, e.g., self-trapping effect [9, 13] and strong oscillatory instabilities [9, 17].

In order to check our conjectures above we proceed to estimate a growth rate from the standard modulation stability analysis of plane waves in one-dimensional arrays [22, 23, 24, 25]. Here, one looks at the dispersion relation of a phonon wave whose amplitude and phase are perturbed by a modulation plane-wave. This yields a dispersion relation that for

decaying small-amplitude waves read as [22, 23, 25]

$$\Omega_Q = 2J \sin(k) \sin(Q) - \sqrt{8J} \times \sqrt{U\psi_0^2 \cos(k) \sin^2(Q/2) + 2J \cos^2(k) \sin^4(Q/2)}, \quad (13)$$

where  $\Omega_Q$  and  $Q$  are the frequency and wavenumber, respectively, of the modulation plane-wave.  $\psi_0$  is the amplitude of the phonon wave. The growth rate  $\Gamma$  of the modulation wave can be estimated from the imaginary part  $\Im(\Omega_Q)$  of Eq. (13), i.e.  $\Gamma \sim \Im(\Omega_Q)$ . Notice that  $\Im(\Omega_Q) \neq 0$  if  $JU \cos(k) < 0$  (bright region) and  $Q \in (0, 2 \arcsin[\sqrt{-U\psi_0^2 \sec(k)/(2J)}])$ .

At first glance, the comparison between a phonon wave modulated by a plane-wave and the single soliton solutions in Eqs. (9) and (10) may appear “strange”. However, both problems are strongly linked [7, 22, 23, 24]. Notice that the modulated phonon wave in Eq. (13) can be seen as infinity train  $\psi = \sum_j \psi_n^B(z - jL)$  of bright solitons, where  $L$  is a distance between the solitons. In Fig. 2 an example of this comparison is shown. Similar construction can be done in the dark region with the help of an infinity train of dark pulses [see Eq. (11)] to emulate a modulated phonon wave.

A simple estimation of  $\Im(\Omega_Q)$  for bright solitons [Eq. (9)] can be done by assuming in Eq. (13) that  $\psi_0$  is the soliton amplitude [ $\psi_0 \equiv \sqrt{4J \cos(k)(\epsilon_0 - 1)/(-3U)}$ ] and  $Q$  is proportional to the inverse width [ $Q \equiv \sqrt{(\epsilon_0 - 1)}$ ]. We note that the approximate estimation of  $Q$  can be done by comparing the envelope shape of a half-cycle oscillation of the modulation wave with the shape of the bright-soliton envelope (see Fig. 2).

Notice that the case  $\Im(\Omega_Q) = 0$  (dark region:  $U \cos(k) > 0$ ) means that plane waves are stable. However, if one tries to extend this conclusion for solitons, one would wrongly conclude that dark solitons are stable. This wrong notion would imply that MI effect is negligible in the dark region, which contradicts the fact that approximate dark solitons can be systematically derived. Moreover, instability for staggered dark solitons have been numerically predicted [16]. Hence, we can conclude that the usual modulation stability analysis, Eq. (13) [7, 22, 23, 24], is not appropriate for deriving conclusions on the stability of solitons in the dark region.

It has been argued that the staggering transformation ( $k \rightarrow \pi - k$ ) in Eq. (13) may overcome this problem. However, as mentioned above, by using this transformation the conditions for the bright and dark regions are also automatically interchanged. In other words, with this transformation one changes from one bright region to other bright region.

So, in the present case the staggering transformation in combination with the usual modulation stability analysis cannot analytically describe MI effect on moving solitons in the dark region.

The remaining question is: how the MI effect for moving solitons can be analytically described in the dark region? In order to investigate this question, in the following, we numerically estimate the growth rate associate with the MI strength for both the bright and the dark regions. Afterwards, we compare numerical results with estimations from the standard modulation stability analysis and from the term  $\eta$  in Eq. (12). We note that the analysis in the bright region is presented only for completeness, and in order to compare with results obtained in the dark region.

From numerical simulations in Fig. 1 we can observe that the growth rate depends on the time,  $\Gamma = \Gamma(t)$ , in a non-trivial form. In fact, the exponential-like nature of the MI effect observed in the probability density,  $\rho_n = |\psi_n^B|^2$ , can be described by a exponential function of the form  $\rho_n \sim \exp(-2 \int_0^t \Gamma dt')$ .

The growth rate can be estimated in simulations by using the expression  $\Gamma(t) = -d\rho_{max}(t)/(2\rho_{max}(t)dt)$ , where  $\rho_{max}(t) = \int_{t-T/2}^{t+T/2} \max(\rho_n(t))dt'/T$  is an average in time of the maximum of  $\rho_n$ . This average is used to smooth out small oscillations of  $\rho_n$  due to the discreteness of the system and is valid for  $t \geq T/2$ . Here  $T$  is a small time scale, i.e.  $2/T \gg \Gamma(T/2)$ . Notice that these small oscillations in time of the solitons have been discussed in Ref. [11].

Since the analytical estimation of the growth rate [ $\Gamma \sim \Im(\Omega_Q)$ ] can be done only for the initial soliton form, we perform a comparison only for a short initial time scale, namely  $t = T/2$ .

In Fig. 3 we show the numerical estimations of the initial  $\Gamma$  value, i.e.  $\Gamma(T/2)$ , for the bright region . A comparison with the analytical from the standard modulation analysis is also presented. We observe that except for a constant factor ( $\kappa_1 = 0.4$ ) the analytical approximation  $\kappa_1 \Im(E_Q)$  describes qualitatively well the behavior of the growth rate. In particular, in Fig. 3a it is possible to observe that the strength of the MI effect reduces as the soliton width (amplitude) increases (decreases), i.e.  $\epsilon_0 - 1 \rightarrow 0$ . In Fig. 3b estimations of the growth rate for the first Brillouin zone are presented, showing that MI effects become weak as  $|\cos(k)| \rightarrow 0$ , but they do not completely vanish as predicted by the theory. However,  $\Gamma$  tends to be negligible for very small amplitude solitons, i.e  $\epsilon_0 \simeq 1$ ,  $k \simeq \pi/2$ . Notice that

qualitative predictions from  $\eta$  [Eq. (12)] are identical to the standard modulation analysis in the present case.

Now we consider the case of MI effect on solitons in the dark region ( $JU \cos(k) > 0$ ), where Eq. (13) does not provide any information. However, since we have found approximate dark soliton solutions, we should expect also MI effects here. Besides, since  $\eta$  [Eq. (12)] is equal in both regions, we can expect that the behaviour MI strength on pulse solitons in the dark region is similar to that in the bright region.

Notice that in order to obtain more information about the MI effect on solitons, it is convenient to compare both the bright and dark regions. An *exact* quantitative comparison of a bright soliton [Eq. (9)] with a dark pulse,  $u_n$  [Eq. (11)], is not possible, since their envelopes cannot not be exactly equal. So, for the sake of comparison and before we characterize the dark pulses  $u_n$ , we define a sech pulse in the dark region as  $u_n^{test} = i\psi_n^B$ . Here  $i$  is the imaginary unit and  $\psi_n^B$  is given in Eq.(9). This pulse is identical to a bright soliton, except that the relation  $JU \cos(k) > 0$  can be considered.

In Fig. 4a and 4b we show numerical estimations of  $\Gamma$  vs.  $\epsilon_0 - 1$  and  $k$ , respectively, for  $u_n^{test}$ . The same cases as in Fig. 3 are considered here too. We observe that Fig. 4 is qualitatively similar to Fig. 3. However, the  $\Gamma$  values in the dark region (Fig. 4) have a factor  $\sqrt{2}$  larger than in the bright region (Fig. 3). At first glance, it is a surprising result, taking into account that plane waves in the dark region are stable. However, it is straightforward to observe that  $\eta \sim A_B/2$  or  $\eta \sim A_D/\sqrt{2}$ , where  $A_B$  and  $A_D$  are the bright [Eq. (9)] and dark [Eq. (10)] amplitudes, respectively. It means that for identical bright and dark pulses with equal amplitude ( $A_B = A_D$ ), as in Figs. 3 and 4, the MI strength, represented by  $\eta$  is  $\sqrt{2}$  times higher in the dark region than in the bright one. It also means that in order to obtain in the dark region a quantitative similar MI result than in Fig. 3 (bright region), one can define a sech pulse in the dark region but with the amplitude and width of the dark soliton [Eq. (10)], regardless of the soliton form. This assumption can be straightforwardly corroborated by numerical simulations.

The results above show that the strength of the MI effect in the bright and dark regions is different. And this difference cannot be estimated with the usual standard modulation stability analysis in combination with the staggering transformation. Moreover, it shows that the approximate soliton solutions, in fact, do contain information regarding their modulation instability. To the best of our knowledge, this type of analysis for moving solitons in the

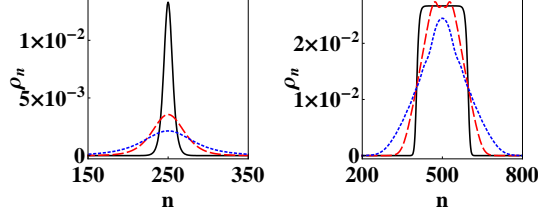


FIG. 5: (Color online) Snapshots of the probability density  $\rho_n$  of a Bright (left panel) and dark (right panel) breathers at different times [ $t = 0$  (solid line), 200 (dashed line), and 400 (dotted line)].  $J = 1$ ,  $U = -1$ ,  $|\epsilon_0 - 1| = 0.01$ ,  $k = 0$  (left panel), and  $k = \pi$  (right panel).

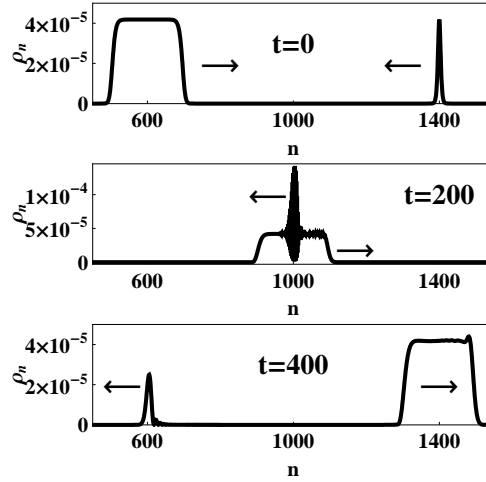


FIG. 6: Snapshots of the probability density  $\rho_n$  of a collision between a bright soliton [Eq. (9)] and a dark pulse [see Eqs. (11) and (10)] at different times (top-bottom:  $t = 0, 200$ , and  $400$ ). Arrows indicate direction of motion: “ $\rightarrow$ ” for the dark pulse and “ $\leftarrow$ ” for the bright soliton.  $k = 0.49\pi$  (bright),  $k = 0.51\pi$  (dark),  $\epsilon_0 = 1.02$  (bright),  $\epsilon_0 = 0.99$  (dark),  $J = 1$ , and  $U = -1$ .

dark region and in the whole first Brillouin zone has not been reported, so far.

For completeness in Figs. 5 and 6 snapshots of the probability-density evolution of solitons [Eq. (9)] are dark pulses [Eq. (11)] are shown. In particular, in Fig 5 two breather cases ( $|\cos(k)| = 1$ ) for the bright (Fig. 5a) and dark region (Fig. 5b) are shown. we observe the usual broadening of the pulse and the decaying of the amplitude at different time scales. It is important to remark that in the case of the dark region (Fig. 5b) the collapse of the breather starts from the lateral sides, and then moves to the center. Notice that the breather maximum does not decay immediately but when the collapse process reaches the center.

In Fig. 6 an example of a collision between a high-velocity bright soliton and dark pulse

is shown. We observe that those high-velocity solitons are stable against collisions and they are less prone to MI effect, as expected from the analysis done for 3, and 4.

For very long time scales solitons in Fig. 6 undergo similar collapse as for the breather case in Fig. 5. We note that the small amplitude radiation observed in Fig. 6 have been investigated with great detail in Refs. [5].

Since, the solitons from Eqs. (9) and (10) undergo only “self-defocusing” instability, we can conclude that these solutions pose an analytical upper boundary for “defocusing-like” solitary waves of the DNLSE. So, solitary waves with higher amplitudes can undergo other instabilities as the oscillatory or the self-trapped [9, 13, 17].

Finally, we note that the soliton solutions in Eqs. (9) and (10) vanish at  $|k| = \pi/2$ . This value, known as the “zero-dispersion” point, has been examined with great detail in Ref. [14].

#### IV. CONCLUSIONS

Motivated by the problem of coherent matter wave transport in BEC arrays, within the first-band approximation, we have studied anew the problem of modulation instability (MI) of small-amplitude solitary waves in the discrete Schrödinger equation (DNLSE). For that we have developed a self-contained quasicontinuum approximation (SCQCA) for the DNLSE to derive approximate analytical soliton solutions. We have used the well-known notion that solitons can be considered as a signature of the MI to conjecture that analytical soliton solutions following from the approximate integration of the system contain already qualitative information of the MI strength on the solitons when propagating. We have shown with the help of numerical simulations that this conjecture describes qualitatively well the “self-defocusing” MI effect of small-amplitude solitons in the dark region where the standard modulation stability analysis of planewaves and/or the staggering transformation do not provide any information. Though planewaves are stable in the dark region, we have shown that for identical pulses in the bright and dark region the strength of the “self-defocusing” MI is higher in the dark region than in the bright one. This fact was shown not only numerically but also by following the conjecture posed above.

Since the soliton solutions derived here only present “self-defocusing” instability, their amplitudes can be considered as analytical upper boundaries for this instability.

Last but not the least, the analysis proposed here can be straightforwardly extended to higher spatial dimensions (work in progress) where the motion of solitary waves and vortices can be also observed and analyzed.

- 
- [1] R. A. Vicencio, J. Brand, and S. Flach, Phys. Rev. Lett. **98** (2007), 184102.
  - [2] T. Schumm, S. Hofferberth, L. M. Andersson, S. Wildermuth, S. Groth, I. Bar-Joseph, J. Schmiedmayer and P. Krüger, Nature Phys. **1** (2005), 57.
  - [3] A. Kay, J. K. Pachos, and C. S. Adams, Phys. Rev. A **73** (2006), 022310.
  - [4] N. S. Ginsberg, S. R. Garner and L. Vestergaard Hau, Nature **445** (2007), 623.
  - [5] O. F. Oxtoby and I. V. Barashenkov, Phys. Rev. E. **76** (2007), 036603.
  - [6] A. A. Vakhnenko and Yu. B. Gaididei, Theor. Math. Phys. **68**, 873 (1986).
  - [7] Yu. S. Kivshar and D. K. Campbell, Phys. Rev. E **48** (1993, 3077).
  - [8] Ch. Claude, Yu. S. Kivshar, O. Kluth, and K. H. Spatschek, Phys. Rev. B **47** (1993), 14228.
  - [9] A. B. Aceves, C. De Angelis, T. Peschel, R. Muschall, F. Lederer, S. Trillo, and S. Wabnitz, Phys. Rev. E **53** (1996), 1172.
  - [10] J. Gómez-Gardaños, L. M. Floría, M. Peyrard, and A. R. Bishop Chaos **14** (2004), 1130.
  - [11] M. J. Ablowitz, Z. H. Musslimani, and G. Biondini, Phys. Rev. E **65** (2002), 026602.
  - [12] M. Peyrard, Nonlinearity **17** (2004), R1.
  - [13] A. Trombettoni and A. Smerzi, Phys. Rev. Lett. **86** (2001), 2353.
  - [14] D. Pelinovsky and V. M. Rothos, Physica D **202** (2005), 16.
  - [15] Y. S. Kivshar, W. Królikowski, and O. A. Chubykalo, Phys. Rev. E **50** (1994), 5020.
  - [16] M. Johansson and Y. S. Kivshar, Phys. Rev. Lett. **82** (1999), 85.
  - [17] B. Sánchez-Rey, M. Johansson, Phys. Rev. E **71** (2005), 036627.
  - [18] F. S. Cataliotti, S. Burger, C. Fort, P. Maddaloni, F. Minardi, A. Trombettoni, A. Smerzi, M. Inguscio, Science **293** (2001), 843.
  - [19] A. Smerzi and A. Trombettoni, Phys. Rev. A **68** (2003), 023613.
  - [20] G. L. Alfimov, P. G. Kevrekidis, V. V. Konotop, and M. Salerno, Phys. Rev. E **66** (2002), 046608.
  - [21] R. Carretero-González, D. J. Frantzeskakis, P. G. Kevrekidis, Nonlinearity **21** (2008), R139.
  - [22] Y. S. Kivshar and M. Peyrard, Phys. Rev. A **46** (1992), 3198.

- [23] I. Daumont, T. Dauxoix, and M. Peyrard, *Nonlinearity* **10** (1997), 617.
- [24] V. V. Konotop and M. Salerno, *Phys. Rev. A* **65** (2002), 021602(R).
- [25] Falk Lederer, George I. Stegeman, Demetri N. Christodoulides, Gaetano Assanto, Moti Segev and Yaron Silberberg, *Phys. Rep.* **463** (2008), 1.
- [26] D. E. Pelinovsky, P. G. Kevrekidis, and D.J. Frantzeskakis, *Physica D* **212** (2005), 1.
- [27] A. Neuper, F. G. Mertens and N. Flytzanis, *Z. Phys. B* **95** (1995), 397.
- [28] C. Brunhuber, F. G. Mertens, and Y. Gaididei, *Phys. Rev. E* **73** (2006), 016614.
- [29] E. Arévalo, *Phys. Rev. E* **76** (2007), 066602.
- [30] E. Arévalo, *Europhys. Lett.* **83** (2008), 10004.
- [31] E. Arévalo, *Phys. Rev. Lett.* **102** (2009), 224102.